

Grain-size trends, basin subsidence and sediment supply in the Campanian Castlegate Sandstone and equivalent conglomerates of central Utah

Ruth A. J. Robinson and Rudy L. Slingerland

Department of Geosciences, Pennsylvania State University,
University Park, PA 16802, USA

ABSTRACT

Reconstructions of grain-size trends in alluvial deposits can be used to understand the dominant controls on stratal architecture in a foreland basin. Different initial values of sediment supply, tectonic subsidence and base-level rise are investigated to constrain their influence on stratal geometry using the observed grain-size trends as a proxy of the goodness of fit of the numerical results to the observed data. Detailed measurements of grain-size trends, palaeocurrent indicators, facies and thickness trends, channel geometries and palynological analyses were compiled for the middle Campanian Castlegate Sandstone of the Book Cliffs and its conglomerate units in the Gunnison and Wasatch plateaus of central Utah. They define the initial conditions for a numerical study of the interactions between large-scale foreland basin and small-scale sediment transport processes. From previous studies, the proximal foreland deposits are interpreted as recording a middle Campanian thrusting event along the Sevier orogenic belt, while the stratal architecture in the Book Cliffs region is interpreted to be controlled by eustatic fluctuation with local tectonic influence. Model results of stratal geometry, using a subsidence curve with a maximum rate of $\approx 45 \text{ m Myr}^{-1}$ for the northern Wasatch Plateau region predict the observed grain-size trends through the northern Book Cliffs. A subsidence curve with a maximum rate of $\approx 30 \text{ m Myr}^{-1}$ in the Gunnison–Wasatch Plateaus best reproduces the observed grain-size trends in the southern transect through the southern Wasatch Plateau. Eustasy is commonly cited as controlling Castlegate deposition east of the Book Cliffs region. A eustatic rise of 45 m Myr^{-1} produces grain-size patterns that are similar to the observed, but a rate of eustatic rise based on Haq *et al.* (1988) will not produce the observed stratal architecture or grain-size trends. Tectonic subsidence alone, or a combined rate of tectonic subsidence and a Haq *et al.* (1988) eustatic rise, can explain the stratal and grain-size variations in the proximal and downstream regions.

INTRODUCTION

In this paper, our objective is to illustrate how sediment supply, subsidence and eustasy interact to produce stratal architecture in the coarse-grained fluvial system that deposited the lower Castlegate Sandstone and correlative units in central Utah. Our approach is to perform numerical experiments using an unsteady, nonuniform loose boundary sediment transport model of heterogeneous grain sizes in which: (1) subsidence is imposed using previously published histories (Pang & Nummedal, 1995); (2) grain-size distributions and water discharge are back calculated from outcrop measurements of grain size and channel geometries, respectively; (3) sediment feed rates are varied; and (4) computed results of stratal geometry and vertical and downstream fining patterns

are compared to the observed to eliminate certain combinations of sediment feed rate, subsidence and eustasy.

The results demonstrate that, depending on sediment supply rate, subsidence and eustasy dominate in the upstream and downstream regions, respectively, creating downstream fining and stratal patterns of multiple origin. An intermediate region of rapid changes in grain size and stratal thickness exists where there is a mixed influence of subsidence, base level and sediment supply. The numerical reconstructions also imply that subsidence rates and patterns varied along strike on the Castlegate alluvial plain, being higher in the northern region. These differences are most readily attributable to the influence of previously delineated thrust segments of the central Sevier thrust system (see Villien & Kligfield, 1986; Lawton *et al.*, 1997) and early deformation of the San Rafael uplift in central Utah (Fig. 1).

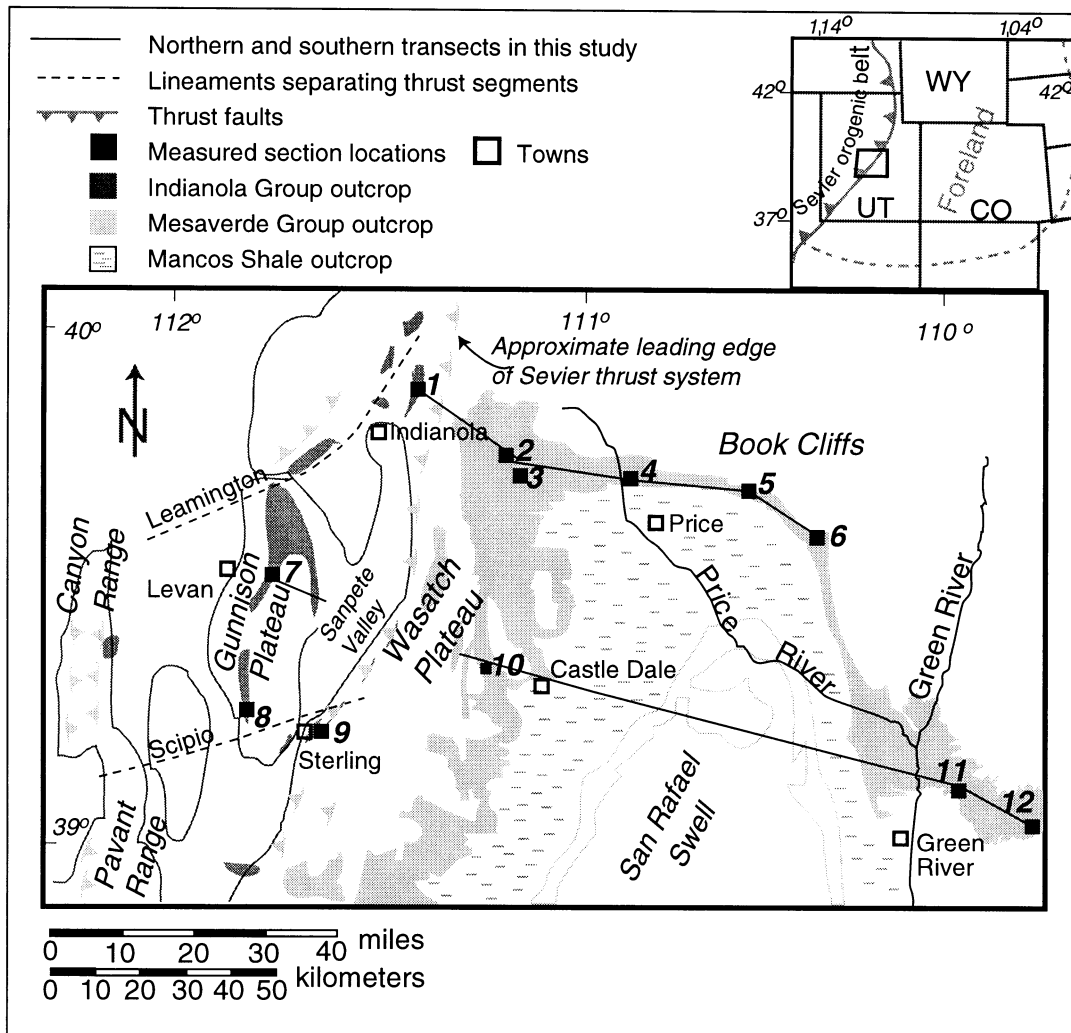


Fig. 1. Location of measured sections, towns and Upper Cretaceous outcrops of central Utah. The inset map shows the field area of central Utah in relation to surrounding states. Numbered locations are: 1, Lake Fork; 2, Bennion Creek; 3, Bear Creek; 4, Price Canyon (Type Locality); 5, Nine Mile Canyon; 6, Sunnyside; 7, Chicken Creek; 8, Mellor Canyon; 9, Sixmile Canyon; 10, Joes Valley Reservoir; 11, Tuscher Canyon; 12, Thompson Canyon.

Background

The middle Campanian Castlegate Sandstone in east-central Utah provides an excellent test of the relative importance of both the rate and the magnitude of tectonic subsidence, eustasy and sediment supply on stratal architecture. The Castlegate Sandstone and correlative units form deposits that extend from the frontal Sevier thrust region to the time-equivalent shoreline over a distance of ≈ 250 km. The coarse- to fine-grained Castlegate Sandstone in the Book Cliffs region contrasts sharply with its correlative cobble conglomerates exposed in the north-central Wasatch Plateau and the boulder-cobble conglomerates of the Indianola Group in the western Wasatch and Gunnison Plateaus (Fig. 1). The basal contact of the Castlegate Sandstone, defining a surface that separates braided river deposits (Pfaff, 1985; Miall, 1993, 1994; Van Wagoner, 1995; Yoshida *et al.*, 1996) from underlying coastal plain and nearshore marine deposits of the Blackhawk Formation (Young, 1955; O’Byrne &

Flint, 1995; Kamola & Van Wagoner, 1995), was first interpreted as a regional disconformity by Spieker (1946). Subsequently, Van Wagoner *et al.* (1991), Olsen *et al.* (1995), Van Wagoner (1995) and Yoshida *et al.* (1996) have interpreted the disconformity as a sequence boundary.

Although there have been several stratigraphic divisions proposed for the Castlegate Sandstone (e.g. Van De Graaff, 1972; Lawton, 1986a; Olsen *et al.*, 1995), the most popular division defined at the type locality in Price Canyon (Fig. 1) is: (1) a cliff-forming, massive sandstone representing braided river deposits (herein termed the lower Castlegate unit); (2) a middle sandstone and siltstone unit that represents finer-grained meandering river deposits (herein termed the middle Castlegate unit); and (3) a second, cliff-forming coarse sandstone representing braided river deposits of the Bluecastle Tongue member (Lawton, 1986a; Van Wagoner *et al.*, 1991; Yoshida *et al.*, 1996). The lower Castlegate unit can be traced down depositional dip well past Thompson Canyon (Fig. 1)

but the middle and upper units are replaced laterally by the Buck Tongue, Sejo Sandstone and Neslen Formation at outcrops east of Horse Canyon (Lawton, 1983; Miall, 1993; Van Wagoner, 1995; Yoshida *et al.*, 1996).

Correlations to the west are hampered by poor exposure but Spieker (1949), Armstrong (1968) and Van De Graaff (1972) recognized the quartz-rich deposits of the lower Castlegate unit as time-equivalent to conglomerates in the eastern Wasatch Plateau (i.e. Bennion Creek locality) and the upper Indianola Group conglomerates of the western Wasatch and Gunnison plateaus and the Canyon and Pavant ranges (Fig. 1). The latter, containing quartzose and carbonate clast-dominated units, are associated with Late Cretaceous thrusting events (Fouch *et al.*, 1983; Lawton *et al.*, 1994; DeCelles *et al.*, 1995; Schwans, 1995) and Lawton (1985) has suggested a potential correlation with the quartzose upper Sixmile Canyon Formation of the Indianola Group.

Although mechanisms controlling deposition of the Castlegate Sandstone are still under debate, Spieker (1946, 1949), Armstrong (1968), Van De Graaff (1972), Fouch *et al.* (1983), Lawton (1985, 1986a), Schwans (1995) and Yoshida *et al.* (1996) emphasize the influence of middle Campanian thrust faulting events in the Sevier orogenic belt on Castlegate Sandstone deposition. In the more distal foreland east of Green River, Van Wagoner (1995) invokes eustatic fluctuations and local tectonic uplift of NW-trending blocks associated with Laramide deformation (Uncompahgre Uplift) as the dominant controls on fluvial deposition. Yoshida *et al.* (1996) suggest that deposition in the Book Cliffs region north-west of Green River is influenced by reactivation of the NW-trending Palaeozoic Paradox Basin.

DESCRIPTION OF THE CASTLEGATE SANDSTONE AND EQUIVALENT CONGLOMERATES

Field observations

Sections were measured in detail along two transects (Fig. 1) to obtain the following information: (1) biostratigraphically useful palynomorph assemblages from fine-grained carbonaceous siltstones; (2) areally weighted grain-size distributions; (3) channel hydraulic geometry; and (4) palaeoenvironments of deposition. This information was integrated to define accumulation rates, average sediment feed rates, along-stream channel pattern and grain-size variations and regional palaeoflow direction.

Correlation of lower Castlegate Sandstone and equivalent conglomerates

Eighty-five samples of carbonaceous siltstone and fine sandstones were collected from the Blackhawk Formation, Castlegate Sandstone and equivalent conglomerate units in order to improve correlations between the Book Cliffs

and Wasatch and Gunnison Plateau deposits. Palynology is a useful correlation tool in the Cretaceous Western Interior because latitudinally dependent pollen zones have been established as regional, biostratigraphic indicators (Nichols & Sweet, 1993; Nichols, 1994). Of these, 16 samples were productive enough to define assemblages and pollen zones. Only two siltstone samples and one coal sample from the conglomerate sections in Bennion Creek and Sixmile Canyon were productive. These samples define a useful suite of palynomorphs that can be grouped into the *Aquilapollenites quadrilobus* Interval zone (*P. thalmani* Anderson, *Proteacidites retusus* Anderson, *Erdtmanipollis procumbentiformis* Samoilovich, *Tricolpites* spp., and *A. quadrilobus* Rouse (Fig. 2) of Nichols & Sweet (1993) and Nichols (1994). Species typical of Late Campanian time, such as *Marsypiletes cretaceous* are rare, and species typical of Latest Campanian–Maastrichtian, such as *Wodehouseia* spp., *Mancicorpus* spp. and *Cranwellia* spp., are absent. Species representative of the lower part of the *A. quadrilobus* Interval zone or upper *A. senonicus* zone, for example *Pseudoplicapollis* spp., are also rare. Therefore, the palynomorphs are assigned to the middle part of the *Aquilapollenites quadrilobus* Interval zone (Fig. 3).

These new data suggest a correlation between the lower Castlegate Sandstone in the Book Cliffs with conglomerates in the Bennion Creek section (Fig. 4) and units assigned to the Price River Formation at Sixmile Canyon (Fig. 5). It should be noted that deposits west of, and including, the western flank of the Wasatch Plateau have been interpreted based on their stratigraphic position with relation to angular unconformities (e.g. Spieker, 1946) before the concept of growth strata was developed (Riba, 1976) and have a variety of informal and formal names. Additionally, discriminating between the quartzose, nonmarine conglomeratic units when exposure is limited is very difficult. Therefore, the units presently termed Price River Formation should not be thought of as time-equivalents of the Book Cliffs Price River Formation.

Our results are consistent with, and augment, previous works of Nichols & Jacobson (1982), Fouch *et al.* (1983), Franczyk *et al.* (1990), Nichols & Sweet (1993), Nichols (1994) and Lawton *et al.* (in press). A lower limit of 79 Ma is recognized for the base of the lower Castlegate unit (Fouch *et al.*, 1983; Obradovich, 1993) from a *Baculites asperiformis* specimen collected near the Utah–Colorado border (Gill & Hail, 1975) (Fig. 3). Biostratigraphic evidence suggests that the basal Castlegate surface is older eastward (Fouch *et al.*, 1983). An upper limit of 77 Ma was inferred for specimens of *B. perplexus* (early form) collected from the Buck Tongue through east Utah (Gill & Hail, 1975). Therefore, the duration of the lower Castlegate is no more than ± 2 Myr in eastern Utah. From the palynological work in this study, the designation of middle *A. quadrilobus* Interval zone to these rocks may limit the lower Castlegate to

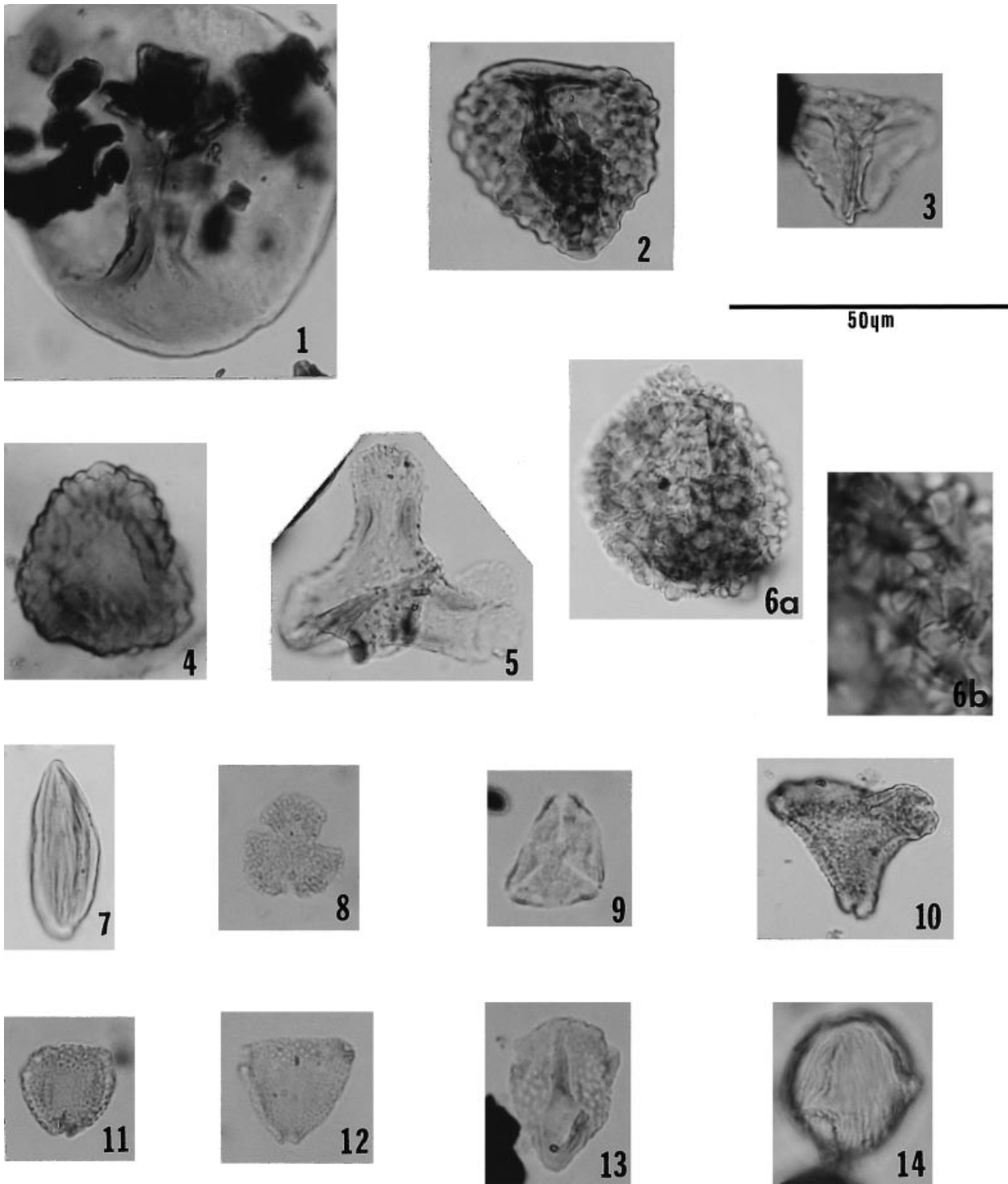


Fig. 2. All specimens are $820\times$ except 6a. 1. *Leiotriletes* spp. 2. *Microreticulatisporites* spp. or *Retitriletes* spp. 3. *Gleichenioidites senonicus* Ross. 4. *Tsugapollenites* spp. (?). 5. *Aquilapollenites quadrilobus* Rouse. 6a. *Erdtmanipollis procumbentiformis* (Samoilovich) Krutzsch. 6b. Same specimen as 6a at a magnification of 1845. 7. *Ephedripites* spp. 8. *Tricolpites interangulus* Newman. 9. *Tricolpites* spp. 10. *Proteacidites retusus* Anderson. 11. *Proteacidites retusus* Anderson. 12. *Proteacidites thalmanii* Anderson. 13. *Striatopollis* spp.

$\approx \pm 1$ Myr and the conglomerate units in Bennion Creek (Fig. 4) and Sixmile Canyon to $\approx \pm 2$ Myr (Fig. 5).

Lawton *et al.* (in press) report a potential late Campanian age for the lower part of the North Horn Formation in Chicken Creek (Fig. 1), which is equivalent

to the Chris Canyon conglomerate of Schwans (1995). Deposits unconformably overlying this unit at the same locality have a late Campanian–early Maastrichtian age (Lawton *et al.*, in press). A bed from the middle Sixmile Canyon Formation of the Indianola Group sampled in

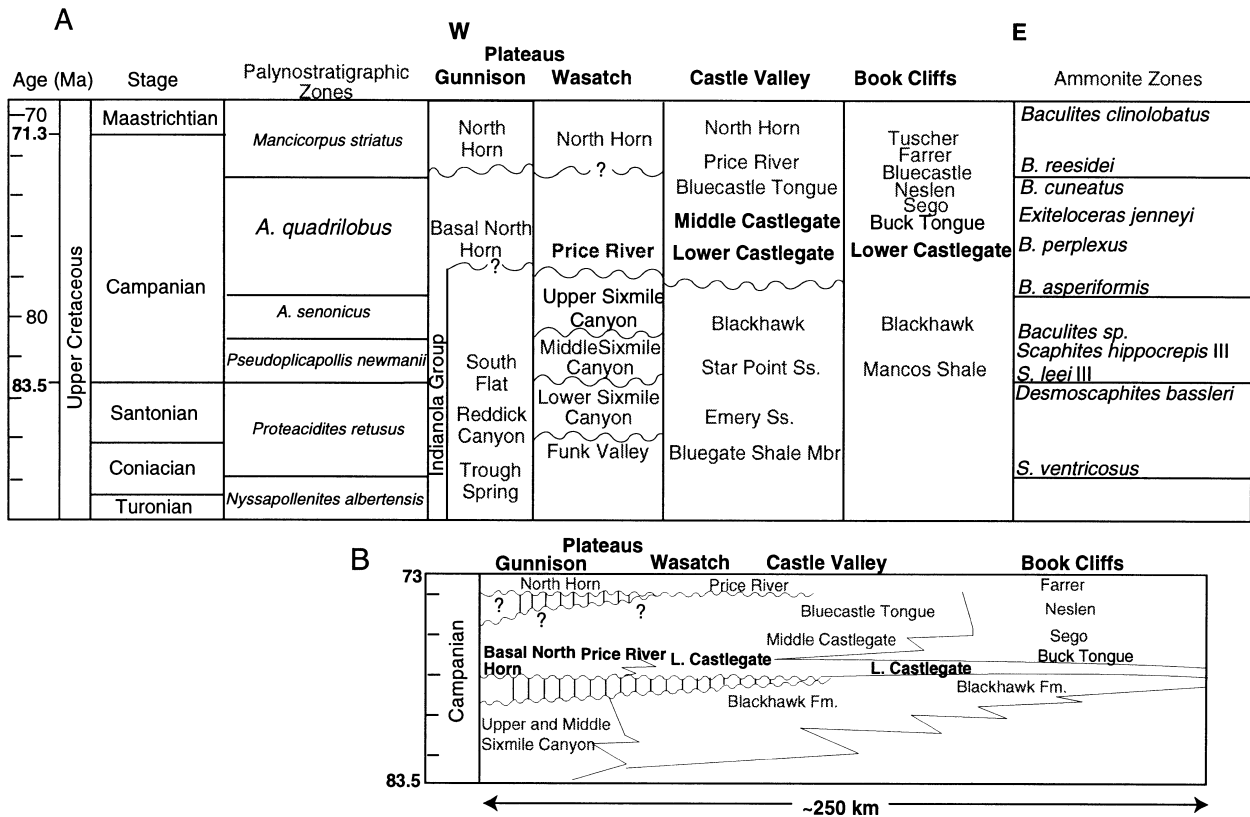


Fig. 3. A. Correlation chart for the Upper Cretaceous units in central Utah, compiled from Obradovich (1993), Fouch *et al.* (1983), Nichols & Sweet (1993), Lawton *et al.* (1994), Nichols (1994), Lawton *et al.* (in press) and this study (s). Time-scale from Obradovich (1993). B. Interpreted Wheeler diagram for Campanian deposits in central Utah (modified from Fouch *et al.*, 1983).

the Hanson Moroni well in Sanpete Valley (Fig. 1) has been dated as Late Cretaceous by Lawton *et al.* (in press) and interpreted as early Campanian by Schwans (1995). The upper part of the Price River Formation in Sixmile Canyon has previously been dated as latest Campanian (Fouch *et al.*, 1983). Since the lower Castlegate is bracketed as middle to early late Campanian, the lower part of the unit assigned to the Price River Formation at Sixmile Canyon and the basal North Horn Formation of Chicken Creek (Fig. 1) are probable equivalents.

Supporting field data for Castlegate correlation

The following data further support the correlation of lower Castlegate Sandstone with the Price River Formation of Sixmile Canyon and basal North Horn Formation (Figs 4 and 5): (1) palaeocurrent indicators; (2) clast lithology of conglomerates; (3) geometry of unconformities; and (4) syndepositional rotation of conglomerate beds (growth strata). Palaeocurrent data in the Book Cliffs and Wasatch Plateau (Lawton, 1986a; Robinson, 1997) illustrate progressive changes in the sediment dispersal direction after lower Castlegate deposition. Data from above the uppermost unconformity at Bennion Creek, Little Bear Creek, Chicken Creek, Sixmile Canyon and Joes Valley Reservoir (Robinson,

1997) all show more easterly to north-easterly directed palaeocurrent indicators. Palaeocurrent indicators in the middle Castlegate and Bluecastle Tongue in the Book Cliffs suggest progressively more northward-directed dispersal systems (Lawton, 1986a; Robinson, 1997). This northerly trend continues into the overlying Price River and North Horn Formations of the Book Cliffs and is interpreted to represent Laramide deformation of the San Rafael Swell in latest Campanian and early Maastrichtian time (Lawton, 1986a).

The clast lithology of the Bennion Creek, Price River (Sixmile Canyon) and basal North Horn conglomerates is distinctive: they are dominated by white, light grey, tan and pink-purple Precambrian Tintic, Caddy and Mutual quartzite clasts (Lawton, 1986a; Robinson, 1997). Lower Castlegate deposits are predominantly composed of clean, well-sorted quartz arenites that contain white, grey and pink quartz grains. Above the top unconformity at Bennion Creek, Little Bear Creek, Chicken Creek and Joes Valley Reservoir, clast lithology becomes more diverse and includes chert, lithic fragments and carbonate clasts, a composition typical of the Price River Formation in the Book Cliffs (Lawton, 1986b; Franczyk & Pitman, 1991; Robinson, 1997). The stratigraphic compositional trends of the upper Indianola Group and Price River – North Horn Formation are well described in Lawton (1986b) and represent the unroofing of Precambrian and

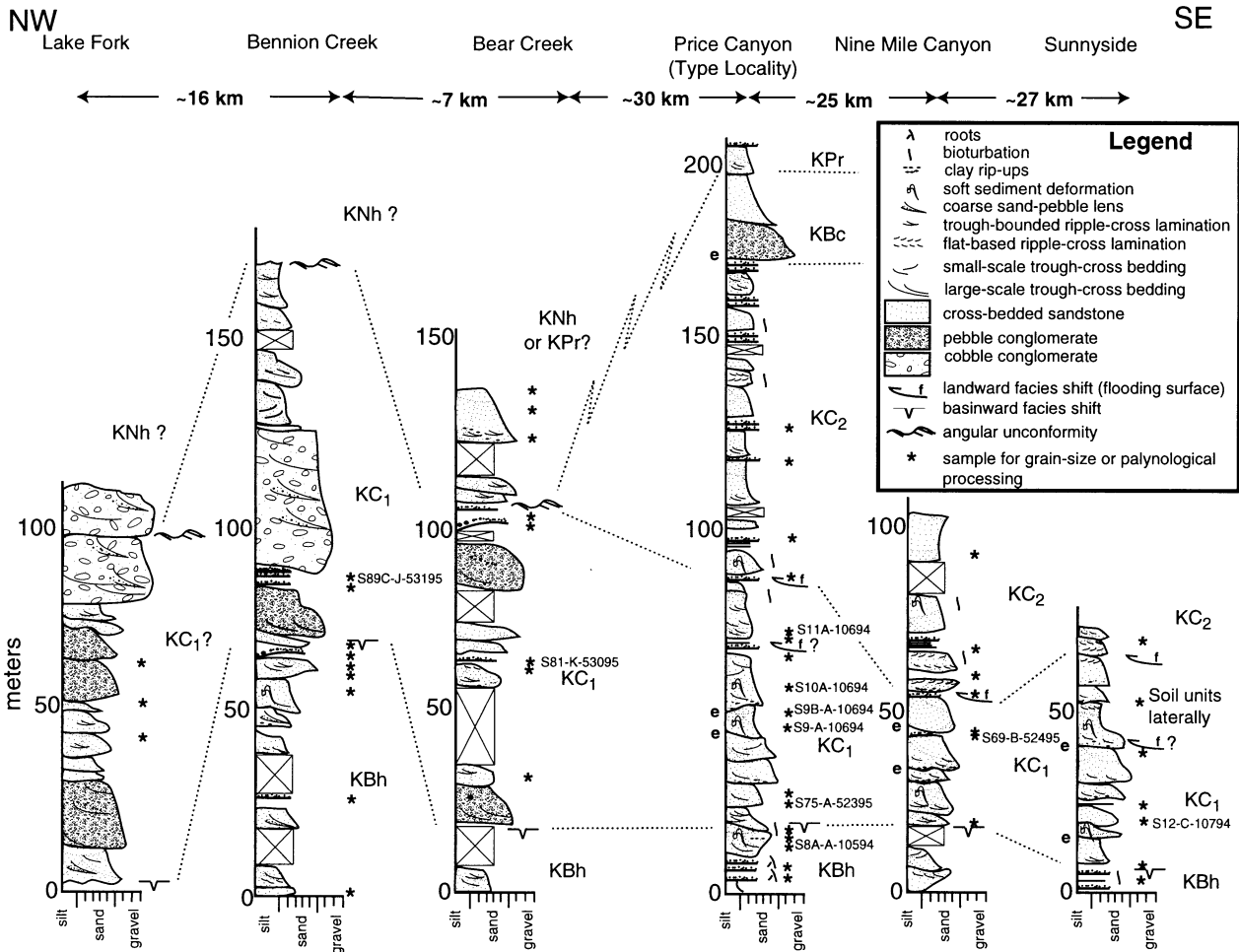


Fig. 4. Measured sections, facies and suggested correlations for the northern transect. Formations are KBh, Blackhawk; KC₁, lower Castlegate; KC₂, middle Castlegate; KBt, Buck Tongue; KPr, Price River; KSX₃, Upper Sixmile Canyon; KNh₁, basal North Horn; KNh, North Horn; KSf, South Flat. Best palynological samples are numbered and the data are tabulated in Table 1.

Cambrian strata of the Canyon Range plate. The vertical compositional variability of these different units is a useful correlation tool and can tie a unit to a specific thrust fault event (Lawton *et al.*, in press).

Deposits above the uppermost angular unconformities at Bennion Creek, Little Bear Creek, Chicken Creek, Sixmile Canyon, Mellor Canyon and Joes Valley Reservoir (Figs 4 and 5) represent landward shifts in lithofacies belts (see also Lawton, 1986a; Franczyk & Pitman, 1991). Additionally, the dip of the underlying conglomerates at Chicken Creek (Lawton *et al.*, in press), Bennion Creek and Little Bear Creek gradually increases by $\approx 10^\circ\text{--}15^\circ$ between the contact with the underlying South Flat and Blackhawk Formations, respectively. These stratal geometries are interpreted as growth strata and result from syntectonic deposition during thrust fault emplacement (e.g. Lageson & Schmitt, 1994; DeCelles *et al.*, 1995; Lawton *et al.*, 1997). These lines of evidence are interpreted as supporting the correlation of the lower Castlegate Sandstone with the conglomerates of the Price River Formation at Sixmile Canyon, the conglomerates

of Bennion Creek and the basal North Horn Formation at Chicken Creek.

Lithofacies description and interpretation

Summary diagrams of the measured sections are presented in Figs 4 and 5. Table 2 defines six lithofacies; additional lithofacies descriptions and interpretations are available in Lawton (1986a), Miall (1993, 1994) and Yoshida *et al.* (1996). Interpretations of depositional environment are discussed below for each transect from north-west to south-east.

Lithofacies interpretations

In the northern transect, the conglomeratic deposits equivalent to the lower Castlegate unit display an association of lithofacies D, E and F (Table 2), organized in two main successions that generally coarsen upwards (Fig. 4). The lower and upper successions are 10–20 m and 25–60 m thick, respectively. Lithofacies D and E are

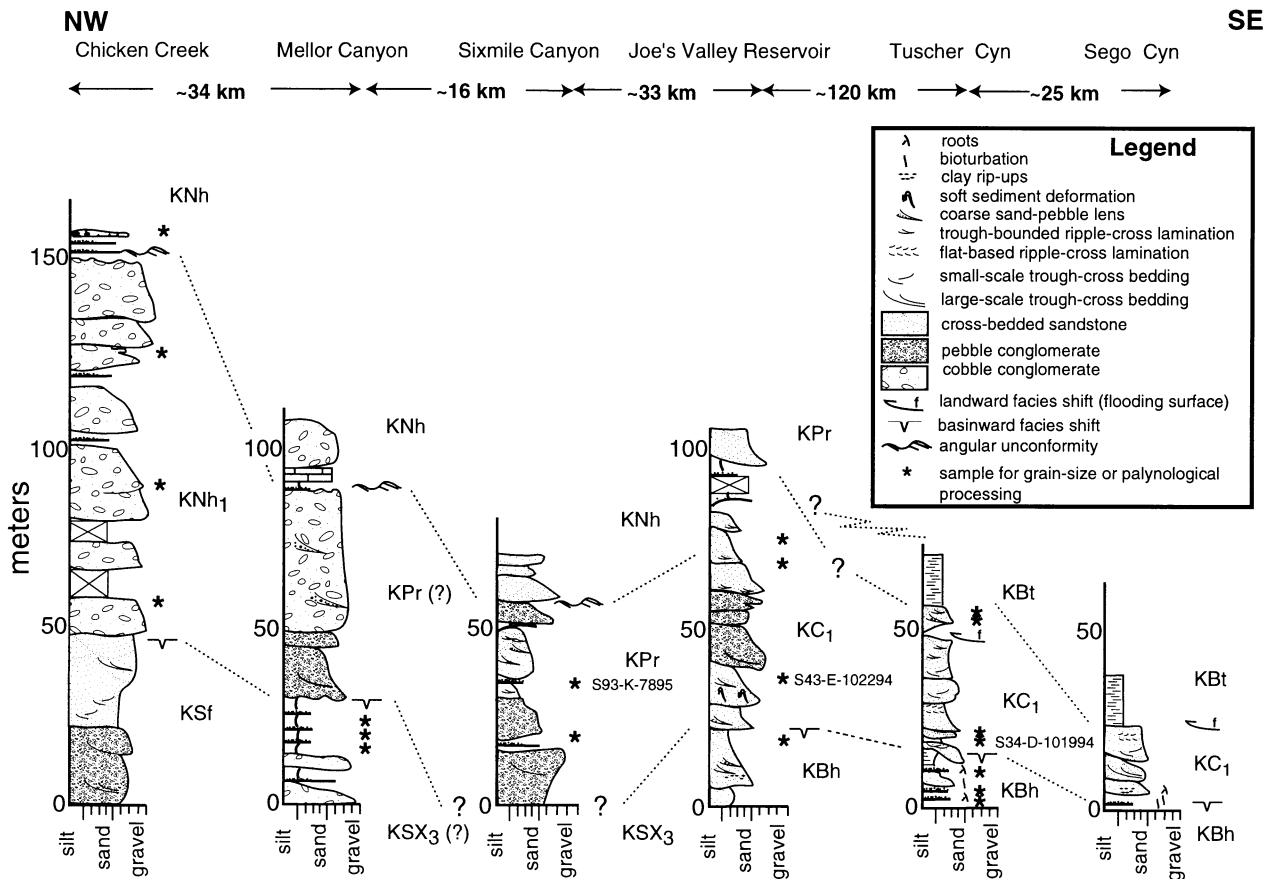


Fig. 5. Measured sections, facies and suggested correlations for the southern transect. See Fig. 4 caption for formation identification.

interpreted to represent channel fill deposits in braided rivers on an alluvial apron. There are minor occurrences of matrix-supported (clays) cobble conglomerate at Bennion Creek and Lake Fork and these represent debris flows. Lithofacies F is well developed at Bennion Creek and Little Bear Creek and represents 3–5-m-thick palaeosol horizons that are erosionally scoured by overlying conglomerate and pebbly sandstone beds. The Book Cliffs sections of the lower and middle Castlegate display two repeating facies motifs, generally organized in two main bed storeys (*sensu* Bridge & Diemer, 1983) of 10–20 m thickness. Lithofacies A and B (Table 2) predominate in the lower Castlegate at all Book Cliffs localities. Lithofacies C occurs at the top of the lower Castlegate at Sunnyside and is present, but less well developed, at Soldier Creek. The association of lithofacies A and B is interpreted here as channel bars and infill within a braided river (large sand-flat bar complexes of Miall (1993), (1994) and Yoshida *et al.*, in press)). Lithofacies A and B are overlain by point bar and crevasse splay deposits of lithofacies C. At the type locality in Price Canyon, lithofacies C defines the base of the middle Castlegate. In the Book Cliffs outcrops, the dominance of lithofacies B, C and F, first occurrences of bioturbation (*Planolites*), flaser bedding, reverse flow indicators and the differences in fluvial architecture, grain size, channel dimensions and sand/mud ratio between the lower and

middle Castlegate units is interpreted as reflecting an increase in tidal influence within a fluvial distributary channel environment.

Along the southern transect, lithofacies D and E predominate in the conglomerate sections of Chicken Creek and Mellor Canyon, are organized in two packages between 20 and 50 m thick and are interbedded with 1–2-m-thick beds of lithofacies A (Fig. 5). This association is interpreted as channel infill within the proximal regions of an alluvial apron. The pebbly and granular deposits at Sixmile Canyon and Joes Valley Reservoir are composed of all six lithofacies. One 20-m-thick pebble conglomerate package of lithofacies D at Joes Valley Reservoir is sandwiched between two 20-m-thick packages of lithofacies A and B. This association is interpreted to represent channel bars and infills, large dunes and vegetated bars of coarse, braided river deposits. At Sixmile Canyon, the base of the Price River Formation is not exposed and two conglomerate packages are present beneath the unconformity below the North Horn Formation. At both Book Cliffs localities of the southern transect, the lower Castlegate Sandstone is overlain by the Buck Tongue of the Mancos Shale. Lithofacies A and B comprise the base and lithofacies C and F occur at the top of the lower Castlegate unit. This contrast in lithofacies between the base and top of the lower Castlegate unit is best developed at Tuscher Canyon.

Table 1.

Specimen identification	S8A-A-10594-10	S9-A-10694	S93-K-7895	S89C-J-53195/4	S8A-A-10594-10B	S75-A-52395	S9A-A-10694	S9B-A-10694	S11A-A-101694	S11B-A-10694	S10A-A-10694	S72A-A-52895	S7A-A-10694	S89C-J-53195/1	S69-B-53195	S81-K-53095
<i>Erdtmanipollis</i> spp.	R			R												R
<i>Proteacidites</i> sp.	▼	▼	▼	▼	▼						▼				▼	▼
<i>Proteacidites retusus</i>			▼								▼					
<i>Proteacidites thalmanii</i>	C	▼														
<i>Erdtmanipollis procumbentiformis</i>	R	R		R												R
<i>Quercoidites</i>																
<i>Tricolpites interangulus</i>		C								▼					R	R
<i>Tricolpites</i> spp.	▼	▼					▼		▼	▼		▼		▼	▼	▼
<i>Appendicorites</i> spp.				▼					▼							
<i>Aquilapollenites quadrilobus</i>			▼	C										C	R	
<i>Aquilapollenites trialatus</i>		R	R													
<i>Ephedripites</i>	R	R						▼						▼		
<i>Sequoiapollenites</i>	R						R				R					
<i>Taxodiaceae</i>	C	C			C				C			C			C	C
<i>Marsypiletes cretaceous</i>		R													R	
<i>Cupuliferoidespollentis</i> spp.	C	C					C									
<i>Tripoporipollenites</i> spp.	C	C							C			C				C
<i>Tricolporipollenites</i> spp.		C														
<i>Cicrisporites</i> spp.	R								R							
<i>Tsugapollenites</i> spp. (?)	R													R		
<i>Poropollenites</i> spp.		R								R						
<i>Sindorapollis</i> spp.		R					R									
<i>Retitriletes</i> spp.		R		R						R						
<i>Rubinella minor</i>																
<i>Leiotriletes</i> spp.			R				R								C	
<i>Striatopollis</i> spp.	R			R						C						
<i>Gleicheniidites senonicus</i>		C		R									R		C	
<i>Gleicheniidites granulatus</i>	C	R														
<i>Psilatritetes</i> spp.	▼			▼							▼					
<i>Densosporites</i> spp.		C	C				▼			C		C				
<i>Dichtyosporites</i> spp.	C															
<i>Stereosporites</i> spp.	C	C	C	▼									C			

Symbols of abundance are: filled triangle indicates >15%; C indicates 5–15%; R indicates <5%.

The uppermost 8–10 m contain flaser bedding, *Ophiomorpha* burrows, thin and irregular-bedded ripple cross-laminated white quartz arenites and a patchily preserved dark grey palaeosol horizon. Below the first occurrence of the Buck Tongue, a distinctive, erosive-based, well-cemented, calcareous, red-weathering white quartz arenite has erosively removed underlying palaeosols. Yoshida *et al.* (in press) have also recognized this suite of deposits. We agree with their interpretation that the top of the lower Castlegate unit represents the onset of a transgression before major flooding deposits the marine Buck Tongue.

Thus, our data support the interpretation that Castlegate aggradation took place in a subsiding foredeep east of an active thrust belt and that the lower Castlegate unit of the Book Cliffs is the foreland equivalent of some of the more proximal foredeep conglomerates in westernmost regions. We now focus on the palaeocurrent and grain-size data collection for these correlated units.

Palaeocurrent data

Palaeocurrent data were collected from the top of the Blackhawk Formation, the lower and middle units of the

Castlegate Sandstone, the Bluecastle Tongue member and the Price River, Sixmile Canyon and basal North Horn Formations (Fig. 6). The measurements are taken from 3-D exposures of large-scale trough cross-strata from the basal parts of main channel fill sequences (defined as a major erosion surface bounding a bed storey by Bridge & Diemer, 1983; Willis, 1993) and, more rarely, from imbricated cobbles within coarse channel fills. Only conglomerate data from the lower Castlegate Sandstone and equivalent units are plotted (Fig. 6). They generally support previous studies of palaeocurrent direction (Van De Graaff, 1972; Pfaff, 1985; Lawton, 1986a; Olsen *et al.*, 1995) and show SE-directed dispersal systems. The palaeocurrent directions in the Book Cliffs differ slightly from those of Van De Graaff (1972) because he summarized the entire Castlegate unit which includes the palaeoflow directions of the Bluecastle Tongue.

The vector means of the palaeocurrent data for the lower Castlegate and proximal conglomerate equivalents are orthogonal to the thrust fronts through central Utah (Fig. 1) and represent consistent transverse drainage patterns (Fig. 6). The best-fitting modern analogue for the lower Castlegate Sandstone and equivalent conglomerates

Table 2.

Facies	Facies description
A	Decimetre- to metre-scale, medium-grained, large-scale trough cross-bedded quartz arenite beds with erosive basal surfaces that are laterally traceable for tens to hundreds of metres. Soft sediment deformation, fossil logs, clay tip-up clasts and carbonaceous matter are common along bases. The tops of sandstone bodies exhibit decimetre sets of small-scale trough cross-bedding or planar cross-stratification
B	Decimetre-scale, medium- to fine-grained quartz arenite. Beds contain small-scale trough cross-strata, ripple cross-lamination, and clay rip-up clasts, and overall fine and thin upwards. Abundant carbonaceous matter in fine-grained material
C	Thin beds of carbonaceous siltstone and fine-grained quartz and lithic arenite containing ripple cross-lamination. These form gently inclined, trough-based packages, tens of metres in width and many decimetres to several metres in thickness. This facies is laterally truncated by sandstone bodies. Local bioturbation and bidirectional ripple cross-lamination. Clay drapes commonly observed in sandstone beds with ripple cross-lamination. Flow indicators diverge from the regional sediment dispersal pattern
D	Decimetre- to metre-scale beds of dominantly well-rounded quartzite pebble conglomerate and granular sandstone arranged in upward-fining successions. Trough cross-stratification in granular sandstones. Conglomerate packages have erosive bases with several metres of scour
E	Well-rounded cobble to boulder quartzite conglomerate in 2–5-m-thick packages with erosive bases. Little vertical grain-size variation
F	Grey, nodular, massive claystone–siltstone. Carbonaceous fragments abundant and some rooting evident.

are the fluvial megafans (Gaghra, Gandak or Kosi) of the modern Ganges foreland basin (Sinha & Friend, 1994), as previously suggested by Van Wagoner (1995). These three systems serve as point sources for sediment and water dispersal into the Ganges foreland along 750 km of the Nepal Himalaya (Gupta, 1997) and ultimately join the strike-parallel Ganges River. Gupta (1997) has recently suggested that prior to segmentation of the Himalayan foreland, drainage in the Ganges foreland was completely transverse to the orogenic front and distributed in approximately 12 rivers. Basin segmentation can produce anticlines that divert stream drainage and produce gridiron, strike-parallel rivers (Tucker & Slingerland, 1996; Gupta, 1997). The consistent palaeo-current patterns of the lower Castlegate unit and subsequent axial drainage and facies shifts observed in the middle Castlegate, Bluecastle Tongue and Price River

(Book Cliffs) and North Horn deposits are consistent with the scenario outlined by Gupta (1997) for the Ganges foreland and are plausible given the thrust style changes after middle–late Campanian time (Lawton, 1986a).

Grain-size measurements

It is important that we estimate the full range of grain sizes in the Castlegate fluvial system because rivers adjust to all the grain sizes supplied from the parent drainage basin, in addition to water discharge, sediment feed rate and subsidence rate (Paola *et al.*, 1992; Cui *et al.*, 1996; Robinson & Slingerland, in press).

Methodology

Grain sizes from separate measurements of (1) channel infills above major erosion surfaces and (2) overlying overbank deposits were collected under the assumption that these deposits represent the main trunk channel of a river system and comprise the full range of grain sizes in transport at any time. Measurements were taken from within a single bed in order to ensure that grains were deposited under similar hydraulic conditions. Data for coarse grain sizes were collected using a 1 × 1-m sampling grid divided into 5 × 5-cm squares. Grains were then randomly selected for measurement if they lay beneath the intersection of two perpendicular strings. Apparent *a* and *b* axes of grains were measured although only the *b* axis is used for modelling as this is the axis that rolls or saltates along the bed. Each sample typically contains 60–80 grain measurements with a range of 30–180 and three samples were taken within each bed. At each section, measurements were made every 2–5 m vertically or more frequently if grain size changed within that distance. In order to test the validity of the *in situ* measuring scheme, the deposit was excavated and all three axes of a clast were measured if the matrix was friable.

For grain sizes smaller than coarse sand, it is difficult to resolve which grains lie under the string crosshairs therefore hand samples were collected for processing in the laboratory. They were disaggregated in a mortar and pestle, sieved and then the percentage of lithics was determined. Any remaining aggregates in the sieves were reprocessed. The final sieved fractions were weighed and a grain-size distribution was calculated. For both grid and hand-sample data, a total outcrop grain-size distribution was calculated as the sum of each bed distribution weighted by bed thickness. These data represent a 'site-specific' distribution. They were, in turn, weighted by half the distance between both the previous and subsequent outcrop to obtain an areally weighted average grain-size distribution for the fluvial system of each transect.

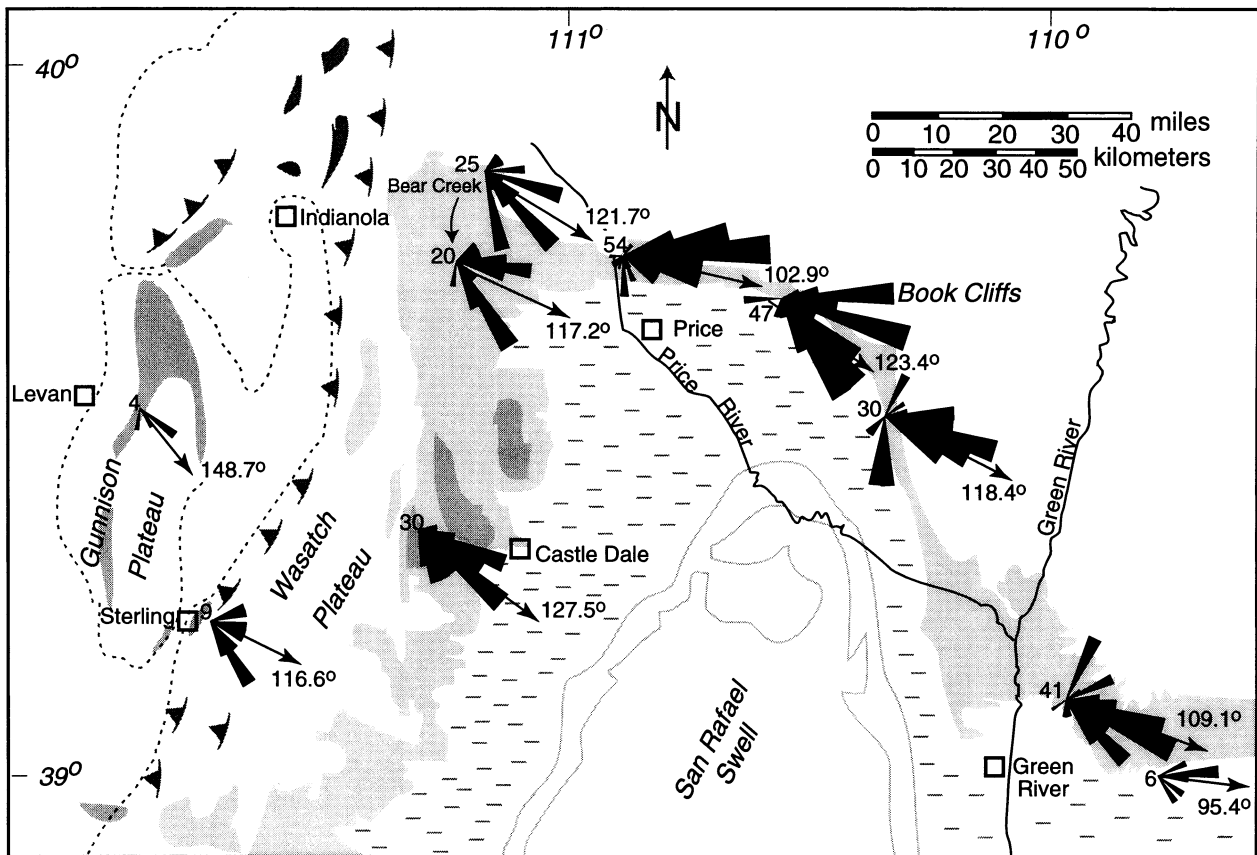


Fig. 6. Palaeocurrent data for the lower Castlegate. See also Lawton (1986a), Olsen *et al.* (1995) and Van De Graaff (1972). Data are plotted in 10° rosette petals with the number of measurements and vector mean.

Results

Figure 7 summarizes the vertical changes in grain size and sorting, and the lateral changes in median size (i.e. Bennion Creek and Bear Creek to Joes Valley Reservoir). In the northern and southern transects, proximal conglomerate sections generally coarsen and thicken up. The more distal sections display increased bed thickness and a small decrease in grain size upward (Figs 4 and 5); this trend is best developed at Price, Tuscher and Thompson Canyons (Figs 4, 5 and 7). The trends in the intermediate sections at Bear Creek, Joes Valley Reservoir and Sixmile Canyon differ from one another (Fig. 7). The deposits at Sixmile Canyon coarsen then fine upwards, at Joes Valley Reservoir coarsen upwards and at Bear Creek fine and then coarsen upwards.

These grain-size data were used to calculate the observed fining rates for both transects. Based on Sternberg's (1875) study of the Rhine River gravels, Barrell (1925) published an expression for grain-size weight reduction as a function of distance. This expression is typically used in a size reduction form (e.g. Lindholm *et al.*, 1979):

$$D_x = D_0 e^{-\alpha x} \tag{1}$$

where D_x represents the maximum size at some distance downstream, x (km), D_0 is the maximum initial size at

$x=0$, and α is the fining rate (km^{-1}). In this study, α is calculated using: (1) the largest median grain size (D_{50}) at each locality; and (2) the weighted mean of all the median sizes (by bed thickness of each measurement at each locality). Thus two fining rates are calculated for each transect by fitting the grain-size trends to an exponential curve (Table 3; Fig. 8). A palinspastic adjustment of 30 km is applied to the Chicken Creek section to account for post-Castlegate deformation (Lawton & Trexler, 1991). The data from Little Bear Creek, Mellor Canyon and Sixmile Canyon are projected onto the transect lines of the northern and southern transects, respectively (Fig. 1).

The areally weighted grain-size distributions for each transect are presented in Fig. 9. Although the southern transect contains a wider distribution of grain sizes, the overall distribution has a slightly smaller D_{50} . However, uplift of the San Rafael Swell makes the southern transect more incomplete. To compensate, we assumed that the grain-size distribution of the missing deposits fell between that of Joes Valley Reservoir to the west and Tuscher Canyon to the east. These missing deposits represent $\approx 25\%$ of the total volume.

Hydraulic data

Channel width measurements were collected where available to provide additional information of the hydraulic

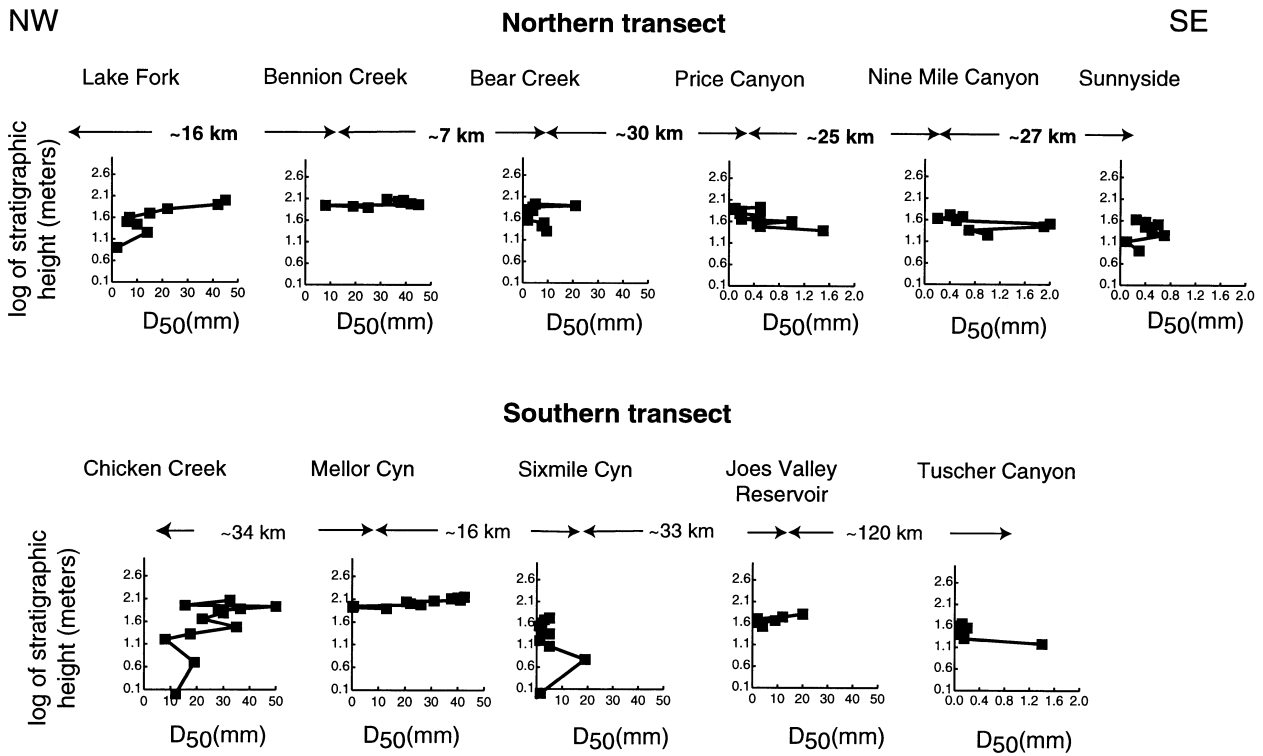


Fig. 7. Northern and southern grain-size trends. Median grain size (D_{50} in mm) for the conglomerate and sandstone deposits vs. stratigraphic height (log scale).

Table 3.

Grain size (D_{50})	Lake Fork	Bennion Creek	Little Bear Creek	Price Canyon	Soldier Creek	Sunnyside	Fining rate, α (km^{-1})
Max (mm)	40	45	9.5	0.27	0.2	0.18	0.063
Mean (mm)	40	19.1	4.3	0.25	0.2	0.16	0.059
		Chicken Creek	Mellor Canyon	Sixmile Canyon	Joes Valley Reservoir	Tuscher Canyon	
Max (mm)		50	42.5	21	20	0.2	0.027
Mean (mm)		25.2	25.5	10.2	8.16	0.18	0.024

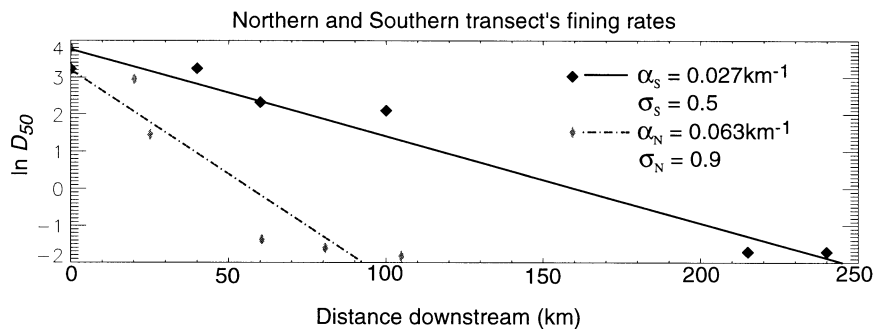


Fig. 8. Observed fining rates for the northern and southern transects using the maximum D_{50} at each locality. The α values represent the slope of the regression line from eqn 1.

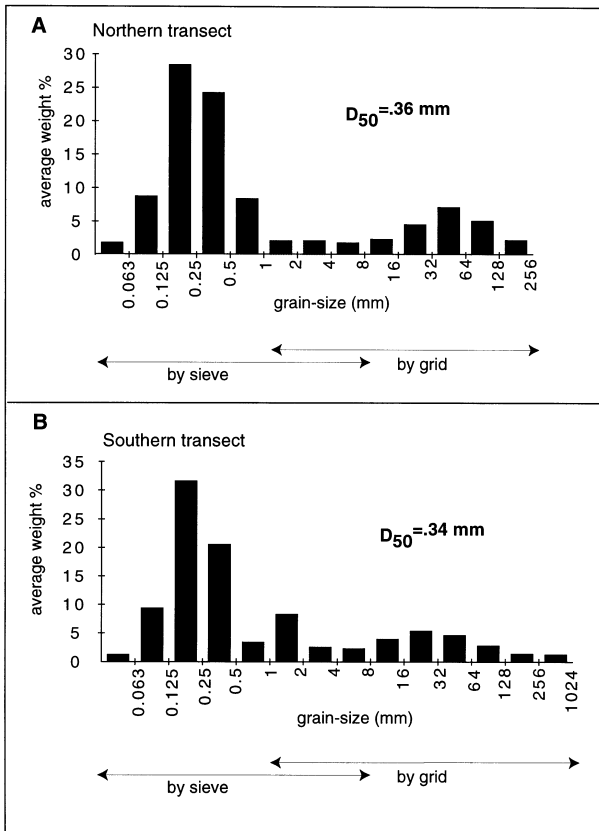


Fig. 9. Total areally weighted grain-size distribution for the (A) northern and (B) southern transects.

setting. Channel width data are used to estimate channel-forming discharge under the assumption that channel width is a function of bankfull discharge (e.g. Bray, 1982). Bridge & Diemer (1983) and Willis (1993) used apparent width measurements of point bars to estimate channel width (multiplying point bar width by 1.33–1.5 (Allen, 1970)). This method, and measurements of total channel width where available, were used in this study. Total channel widths are measured as either the width of a major erosion surface at the top of a bed storey (Bridge, 1993), i.e. the 5th order surface of Miall (1993), or from the width of point bar deposits contained above that surface. These surfaces represent the main channel within the overall channel belt, recognized as being ≈ 3 km in width in the Book Cliffs region (Yoshida *et al.*, 1996). It is recognized that measurements of either channel width or depth are apparent values because they may be of oblique cuts through channels truncated by erosional surfaces. No weighting factor has been applied to the channel width measurements, an assumption that is valid for rectangular channels and is applicable to the flat-based erosion surfaces of the main channels recognized in the lower Castlegate Sandstone. Table 4 summarizes the channel width data and calculations. Given the D_{50} of the bed surface material at each locality and using the average observed width of the channels, and using Bray's (1982) hydraulic geometry equation for channel width as a function of bankfull discharge (Robinson &

Slingerland, in press), estimated bankfull palaeodischarges for each locality can be calculated from

$$Q_w = (0.26W_c D_{50}^{0.07})^{1.89} \tag{2}$$

where W_c is channel width and Q_w is bankfull discharge (Table 4).

Subsidence

In this study, we have used subsidence rates estimated from a 2-D flexural backstripping study of Upper Cretaceous deposits that includes flexural unloading of sediments, decompaction and a water depth correction (Pang, 1994; Pang & Nummedal, 1995). For the east-central region of Utah, early Campanian subsidence rates are estimated to be 45–50 m Myr⁻¹ in the northern Wasatch Plateau region and to decrease exponentially to the east (Pang & Nummedal, 1995; their Fig. 3). However, there is a considerable range in published values. Cross (1986; his Fig. 6C) calculated decreasing rates through time from 134 m Myr⁻¹ between 97 and 74 Ma to 25 m Myr⁻¹ between 74 and 23.7 Ma. In contrast, Heller *et al.* (1986; their Fig. 3C) calculated a subsidence rate of ≈ 25 m Myr⁻¹ from ≈ 85 Ma to ≈ 75 Ma for a location ≈ 75 km east of the Sevier thrust belt in central Utah. Here, we assume that Pang & Nummedal (1995) have adequately captured the distribution of subsidence and use their maximum subsidence rate of ≈ 45 m Myr⁻¹ at the headwaters decreasing downstream to ≈ 20 m Myr⁻¹ in the Book Cliffs. Our subsidence curve is therefore consistent with the Heller *et al.* (1986) calculation for eastern Utah.

Tectonic subsidence in a foreland basin is commonly described as having maximum rate of accommodation space generation in the region adjacent to the thrust belt and a decreasing amount of accommodation space away from the thrust belt (Heller & Paola, 1992; Lageson & Schmitt, 1994; Lawton *et al.*, 1994). In the most proximal regions, this subsidence pattern is complicated by uplift, deformation and remobilization of sediment in a wedge-top depozone (DeCelles & Giles, 1996). All our simulations use the former, simplified form of segmentation of accommodation space.

Sediment supply rate

Given that it is impossible to determine the drainage basin area of the Castlegate streams, it is important to test a range of sediment supply rates to see how different rates affect downstream fining trends. We begin by picking a sediment supply rate that fills the channel volume, calculated as the sum of each section's thickness multiplied by the average channel width at that site, multiplied by half the distance between adjacent sections, over the duration of the deposit. However, the time the river channel of interest is active (T_c) is some fraction of the total duration of the deposit due to avulsion. Therefore, sediment feed rate is calculated as V_c/T_c ,

Table 4.

Northern transect	Lake Fork	Bennion Creek	Little Bear Creek	Price Canyon	Soldier Creek	Sunnyside
Channel width (m)	55 (1)	63.3 (3)	51.6 (3)	94.1 (7)	93.4 (6)	114.6 (4)
Estimated Q_w ($m^3 s^{-1}$)	100.5	119	66	141.7	135.6	193.8
Southern transect	Chicken Creek	Mellor Canyon	Sixmile Canyon	Joes Valley Reservoir	Tuscher Canyon	Thompson Canyon
Channel width (m)	67.5 (2)	90 (1)	115.3 (2)	130.2 (5)	167.7 (6)	232.5 (1)
Estimated Q_w ($m^3 s^{-1}$)	139.2	240	344	415.3	409.5	750

where V_c is integrated channel volume and T_c is a function of avulsion. A channel belt will return to the same location on a floodplain (T_r) in

$$T_r = nP_a(W/m_b) \quad (3)$$

where P_a is mean avulsion frequency, W is floodplain width, m_b is channel-belt width and n varies from 0.3 to 1 (Mackey & Bridge, 1995). If we assume a mean avulsion period of 500 years (Po River is ≈ 490 years averaged over 3000 years; Yellow River is ≈ 600 years averaged over 4200 years (Mackey & Bridge, 1995)), a floodplain width of ≈ 20 km (Hovius, 1996), a channel-belt width of 3 km (Yoshida *et al.*, 1996) and $n=1$, T_r is ≈ 3000 years. This gives an estimate of 285 500 years for T_c . Since this is the least constrained variable in the study, and because of the limited biostratigraphic control, we simulate different sediment feed rates (different T_c values) for both transects (Table 5). No sediment input from tributaries is included because the estimation of grain-size contributions from lateral sources is problematic, although recent studies have shown that downstream

fining in major trunk streams can be significantly affected by tributaries, depending on the tributary sediment feed rate and size distribution (Pizzuto, 1995; Rice & Church, in press; Rice, in press).

Abrasion

Although an additional control on grain-size trends is abrasion (Parker, 1991), quartzose clasts are assumed to be fairly resistant with an experimentally defined abrasion rate that is two or three orders of magnitude smaller than fining rates commonly observed in ancient and modern deposits (e.g. Kuenen, 1956). However, Kodama (1994) has shown experimentally that mechanical breakdown of chert and quartzose material from proximal alluvial fans in Japan may range from 10^{-3} to $10^{-1} km^{-1}$, which is within the range of the measured fining rates in this study. Although the influence of abrasion will have most affect on gravel- and cobble-sized material, our study does not include deposits equivalent to the most proximal fans measured in Kodama's (1994) study and

Table 5.

Variable	Experiment number			
	(1) Northern 1 (2) Northern 2	(3) Northern 3	(4) Southern 1 (5) Southern 2	(6) Southern 3 (7) Southern 4
Water discharge, Q_w	$100 m^3 s^{-1}$	$100 m^3 s^{-1}$	$140 m^3 s^{-1}$	$140 m^3 s^{-1}$
Water increase (x)	Linear increase to $200 m^3 s^{-1}$	Linear increase to $200 m^3 s^{-1}$	Linear increase to $750 m^3 s^{-1}$	Linear increase to $750 m^3 s^{-1}$
Width equation	$w_c = 3.83Q_w^{0.528}D_{50}^{-0.07}$ (Bray, 1982)	Bray (1982)	Bray (1982)	Bray (1982)
Size distribution	See Fig. 9A	See Fig. 9A	See Fig. 9B	See Fig. 9B
Sediment feed rate	(1) $440 kg s^{-1}$ (2) $440 kg s^{-1}$	(3) $660 kg s^{-1}$	(4) $569 kg s^{-1}$ (5) $943 kg s^{-1}$	(6) $569 kg s^{-1}$ (7) $1138 kg s^{-1}$
Subsidence type and rate	exp; $45 m Myr^{-1}$ eustatic rise; $45 m Myr^{-1}$	exp; $45 m Myr^{-1}$	exp; $45 m Myr^{-1}$	exp; $30 m Myr^{-1}$
Hiding coefficient, m	0.65	0.65	0.65	0.65
Length of reach	100 km	100 km	250 km	250 km
Space step	10 km	10 km	10 km	10 km
Timestep	0.5 h	0.5 h	0.5 h	0.5 h
Figure reference	Fig. 10A,B	Fig. 10C	Fig. 11A,B	Fig. 12A,B

so we do not include abrasion as a first-order parameter in this study.

NUMERICAL EXPERIMENTS

Our numerical experiments investigate how stratal patterns are influenced by sediment supply, tectonic subsidence and eustatic rise in base level. The initial conditions for all the simulations as explained above are summarized in Table 5. The calculated grain-size trends (Fig. 8) and total size distribution being fed into the parent rivers for both transects (Fig. 9) are known. Assuming that all the rivers were self-formed and free to adjust to bankfull hydraulic conditions, then the observed channel widths (Table 4) are an estimate of how bankfull discharge changes downstream. In the simulations, sediment and water are fed into the upstream reach until, under the influence of subsidence and changing hydraulic geometry downstream, it reaches steady state at which time the grain-size contours are vertical and constant.

RESULTS AND COMPARISON OF DATA AND MODEL

Experiments 1 and 3 were designed to compare grain-size trends controlled by tectonic subsidence (maximum of 45 m Myr^{-1}) and base-level rise (45 m Myr^{-1}). The distribution and magnitude of accommodation space is different in each case. Base-level rise (or uniform subsidence distribution) produces an equally distributed amount of accommodation space along the profile and therefore, at steady state, sediment is extracted to the bed in equal amounts downstream. Sediment trapping upstream, due to either tectonic subsidence or an increase in accommodation space from base-level rise, means that rivers need to transport a progressively decreasing amount of sediment load across the foreland. However, the downstream rate of extraction of sediment to the bed is different between these two cases. We therefore expect these two end-members to produce different fluvial stratal patterns.

Figure 10 illustrates the temporal evolution of bed elevation with superimposed median grain-size (mm) contours (interval = 10 mm). Bed elevations are relative and only the magnitude of accumulation should be compared between simulations. Each figure presents the fining rate (α) and bed slope decrease rate (β) for the final time-step, where β is calculated from $(S/S_0) = e^{-\beta x}$ and S and S_0 are the slopes at downstream distance x and $x=0$, respectively. From the geometry of the bed elevation lines, it can be seen that accumulation rate decreases downstream in the tectonic case (Fig. 10A), and is equal everywhere in the eustatic case (Fig. 10B). However, the bed slopes necessary to transport sediment in the final time lines are not the same because the profile in expt 1 is progressively lowered due to the subsidence while expt 2's profile continues to build up as base level rises. Although the grain-size trends and fining rates are similar in these two cases, the rate of eustatic rise is

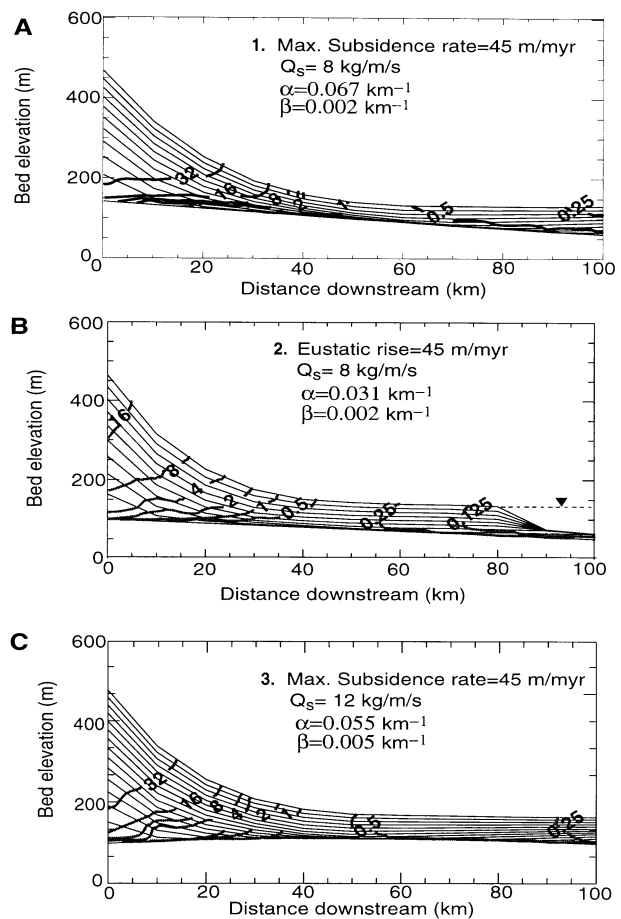


Fig. 10. Results of expts 1, 2 and 3 (Table 5) for the northern transect. Each bed elevation line is equivalent to 250 kyr (A and B) and 150 kyr (C) of basin deposition. Thicker lines are contours of grain size in millimetres.

much higher than any published estimates for the Campanian in Utah (an approximate eustatic rise of $\approx 1.3 \text{ m Myr}^{-1}$ is estimated from the Haq *et al.* (1988) curve for 79–77 Ma). Thus, the observed grain-size and stratal geometry trends are most closely matched with a tectonic subsidence rate of 45 m Myr^{-1} . The initial and final bed slope decrease rate for expt 1 are 0.0015 km^{-1} and 0.002 km^{-1} , respectively. Note that tectonic deflection of the basin also produces a relative base-level rise that influences deposition at the downstream end (Fig. 10A) and causes a slight fining-upwards trend as this region backfills. This trend is associated with a coarsening-upwards trend in the headwaters. These seemingly opposing trends are simply a balance between sediment supply and accommodation space generation. Experiment 3 tests how the stratal patterns adjust to a higher sediment supply rate given the original tectonic subsidence profile. In this case, the river profile aggrades more in order to transport the increased sediment supply. In addition, sediment progrades further into the basin than in expts 1 or 2, the bed slope is higher and there is no fining-upwards trend in the downstream reaches. The calculated sizes at each proximal locality are larger than observed and the fining rate is too low (Fig. 10C). Thus,

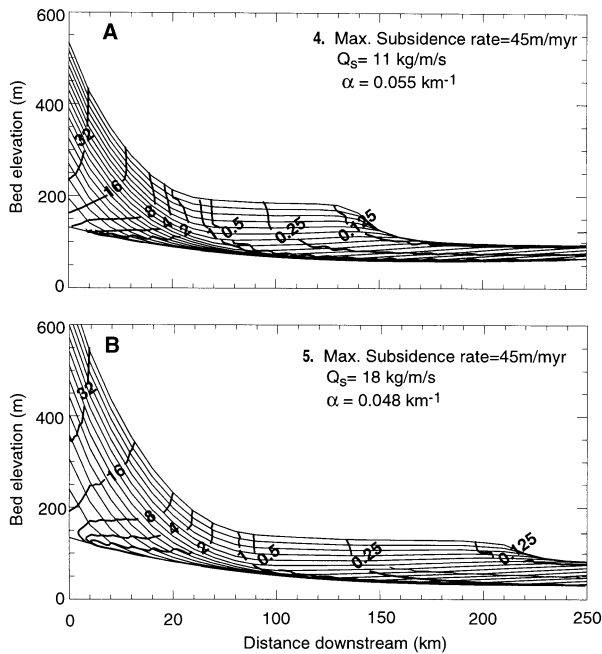


Fig. 11. Results of expts 4 and 5 (Table 5) for the southern transect. Elevation lines are equivalent to 250 kyr of basin deposition.

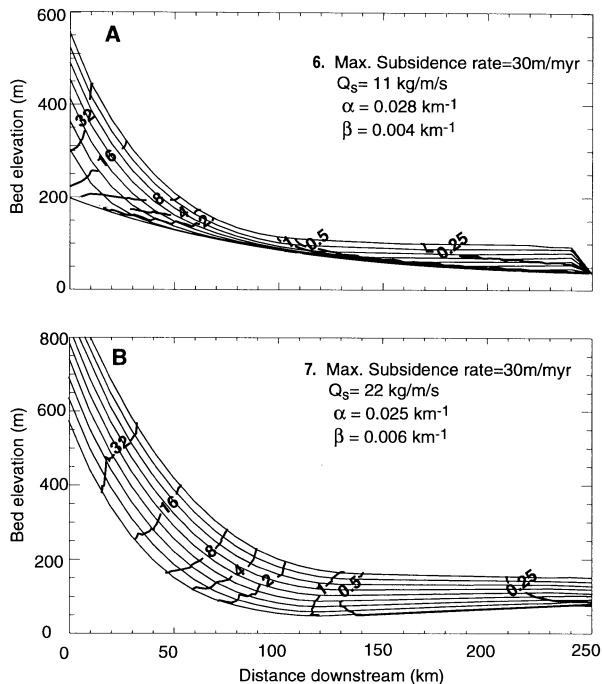


Fig. 12. Results of expts 6 and 7 (Table 5). Elevation lines are equivalent to 250 kyr (A) and 150 kyr (B) of basin deposition.

for the northern transect, a steady-state result is achieved that generally satisfies the observed grain-size trends; a downstream fining rate of 0.063 km^{-1} , upstream regions coarsen upwards and downstream regions fine upwards. This represents a balance between sediment supply and tectonic subsidence for that particular grain-size distribution (Fig. 10A).

The southern transect was also simulated with a

subsidence rate of 45 m Myr^{-1} . To produce the appropriate sedimentary thicknesses in the duration of time allowed, a higher initial bed slope was necessary. The simulated profile illustrates that the basin is underfilled with this subsidence and sediment feed rate combination and the grain sizes do not match the observed trends (expt 4; Fig. 11A). Simulations were performed using other combinations of subsidence and sediment feed rate. Keeping tectonic subsidence rate at 45 m Myr^{-1} and using a higher sediment feed rate (expt 5; Fig. 11B) resulted in too much progradation of sediment into the basin, median sizes being too coarse at the downstream localities and fining too rapidly in the upstream region. Using a lower maximum subsidence rate of 30 m Myr^{-1} and the original sediment feed rate (expt 6; Fig. 11A) reproduces the observed coarser proximal grain sizes and overall downstream grain-size trends in the southern transect (Fig. 11B) but does not reproduce the grain-size trends in the intermediate region about 100 km downstream.

These experiments (1–7) demonstrate that while tectonic subsidence predominantly influences the proximal regions of Castlegate deposition, basin deflection can also influence the downstream reaches of the river profile by creating relative base-level rise. This rise may produce a fining upwards trend, but is dependent on how much sediment progrades to the downstream end which, in turn, is dependent on sediment supply rate and the initial topography of the river profile. For example, expt 3 (higher sediment supply) shows no fining upwards and expt 7 (reduced subsidence and higher sediment supply) displays significantly less fining upwards in the downstream region than the other simulations. Thus, the observed grain-size trends, including the fining-upwards trend in the downstream regions of the southern transect, is replicated with tectonically induced base-level rise only. In both the northern and the southern transects, however, a combined tectonic and eustatic influence would give similar results because the estimated eustatic rise rate (Haq *et al.*, 1988) for the middle Campanian is approximately 15 times smaller than the tectonic influence in the distal region. So although eustatic rise alone cannot explain the grain-size trends and stratal patterns, a combined influence of eustasy and tectonics cannot be discounted.

The southern transect experiments particularly illustrate the relationship between the tectonically dominated region, the downstream base-level-dominated region and an intermediate region where accommodation space decreases rapidly with streamwise distance. During the early stages of the simulation, sediment is trapped in the upstream region producing stratal geometries that thin toward the intermediate region from upstream and downstream, and accumulation becomes quite condensed. In general, depending on such factors as (1) how far from equilibrium a river profile may be (initial topography), (2) the distribution and magnitude of subsidence and (3) the magnitude and size distribution of the sediment feed,

this intermediate region could be an area of erosion while deposition occurs both upstream and downstream. Experiment 7 (Fig. 11) illustrates how increased sediment supply and initial bed slope can reduce the duration of such unconformities in this region. However, in general, a subaerial unconformity could merge both upstream and downstream into correlative conformities (Fig. 11A). Eventually, once the bed slope is adjusted to the sediment supply and subsidence rate in the upstream reaches sediment progrades across this intermediate region and deposition then occurs everywhere along the profile.

Our results suggest that the southern transect region experienced a lower subsidence rate than the northern transect. Additionally, initial and final bed slopes in both simulations suggest that topography was relatively higher in the southern Wasatch Plateau. These differences could be attributed to the onset of San Rafael Swell deformation in the southern Wasatch Plateau (Lawton, 1986a; Franczyk & Pitman, 1991). Alternatively, it is already known that thrust segments are separated along lineaments or transfer zones (Fig. 1) (Lageson & Schmitt, 1994; Lawton *et al.*, in press) and therefore the difference in subsidence rate between these two regions may simply be a reflection of their association with different thrust segments.

DISCUSSION

We have investigated the fluvial stratal patterns and, in particular, the downstream fining produced by tectonic subsidence, eustasy and sediment supply. Our simulations demonstrate that there are significant differences in stratal architecture associated with the different mechanisms of accommodation space generation and therefore that grain-size trends in foreland basins can be used to understand the mechanisms influencing their deposition.

There are immediate implications for synorogenic gravels from this work. As shown recently by Paola *et al.* (1992) and Burbank & Vergés (1994), distribution of orogenic gravels is dependent on structural style, subsidence, sediment feed supply and climate. Our results concur with Burbank *et al.* (1996) by demonstrating that orogenic gravel distribution is also a function of topography because this affects how close a river (or valley) profile is to equilibrium. Our experiments have illustrated how sediment trapping in the proximal region is a function of all the controlling variables mentioned above, but most particularly, the interaction of sediment supply and accommodation space generation. Once the proximal accommodation zone is filled, sediment can rapidly prograde into the foreland because accommodation space is low and sediment flux is high enough to transport the load. If an exponential subsidence profile is a reasonable assumption for foreland basins, then the accommodation space in the distal foreland is not only less, but fairly constant. The intermediary and distal region would be characterized by coarse, thin 'sheets' of sediment. In a recent summary of the Sevier orogenic belt, Lageson &

Schmitt (1994) cautioned against attributing tectonosedimentary significance to conglomerates without knowledge of structural and geomorphic influences. However, it is our hypothesis that, in general, any gravels preserved by tectonic subsidence (or eustasy) leave a distinct downstream fining signature, which can be distinguished from the more irregular signal of 'antitectonic' gravels that may be the result of uplift and rejuvenation of proximal foreland deposits (Heller & Paola, 1992).

Several of the known important geomorphological and crustal processes and feedbacks that influence mountain belts and foreland basin development are missing from the modelling approach. Our streams are 1-D and have constant values of water, sediment and subsidence through time. This is clearly a simplification and can be improved with more complete chronostratigraphic data and subsidence histories. Simulating ancient fluvial deposits requires several assumptions of basin size that are estimated from modern orogens and may not be applicable to the Sevier foreland. Tucker & Slingerland (1996) have demonstrated that sediment feed rate into ancient forelands is controlled by uplift and erosion rate and can be out of phase with the deforming event. We have assumed that thrusting and sediment delivery to the basin are in phase and uninterrupted. More realistic geometries of proximal foreland basins (DeCelles & Giles, 1996), including a foreland-sloping ramp which increases the ability of rivers to transport coarse material into the foredeep, would increase the distance that gravels can prograde. Sediment loading affects the distribution of subsidence and therefore accommodation space (e.g. Flemings & Jordan, 1989) but is not included here.

CONCLUSIONS

The data collected in this study, combined with previously published data, establish the correlation of lower Castlegate deposits with the conglomerates of Bennion Creek, the Price River Formation at Sixmile Canyon and the basal North Horn at Chicken Creek. Numerical modelling results of grain-size trends define a set of possible initial conditions for the Castlegate parent rivers. The northern transect observed grain-size and stratal trends are compatible with an exponential subsidence rate that had a maximum value of 45 m Myr^{-1} in the northern Wasatch Plateau and decreased to 20 m Myr^{-1} in the Book Cliffs region (over 105 km). The rivers had channel widths that ranged on average from $\approx 55 \text{ m}$ to $\approx 114 \text{ m}$ over the same distance and transported a sediment feed rate of $\approx 440 \text{ kg s}^{-1}$. If subsidence rate was in fact higher or lower, sediment feed rate would have to be adjusted by the same amount to maintain the grain-size trend result; initial and final bed slopes would then differ. Within the following ranges, individual adjustments of subsidence rate ($40\text{--}50 \text{ m Myr}^{-1}$) and sediment feed rate ($380\text{--}480 \text{ kg s}^{-1}$) would still give acceptable results. The southern transect observed grain-size and stratal trends are consistent with a maximum exponential

subsidence rate of 30 m Myr^{-1} (± 7) in the Gunnison Plateau that decreased to 11 m Myr^{-1} in the Book Cliffs region (250 km), channel widths that ranged from $\approx 68 \text{ m}$ to $\approx 233 \text{ m}$, and transported a sediment feed rate of 1138 kg s^{-1} (± 100). Improved results for this transect may be obtained by increasing the sampling of grain sizes and the number of sections measured in the Wasatch and Gunnison Plateau regions.

Our results demonstrate that although upstream reaches of rivers draining orogenic belts are most strongly influenced by subsidence, stratal geometry in the intermediate region is influenced by a balance between decreasing subsidence and sediment flux, while downstream reaches are influenced by an almost constant subsidence rate and accommodation space due to relative base-level rise. Grain-size trends are an easily measurable property of all sedimentary rocks and can be used to understand the genesis of stratal geometries and the mechanisms influencing deposition within a sedimentary basin.

ACKNOWLEDGEMENTS

We are grateful to Richard Alley and Peter Flemings for their insightful and rigorous comments on an earlier version of this paper, to Tim Lawton and Paul Heller for their critical reviews, to Kevin Furlong for unlimited use of the IBM RS/6000 computers in the Penn State Geodynamics Computing Laboratory and to Al Traverse for his help and use of the Penn State Palynology Lab. This work was funded by the Petroleum Research Fund PRF-27835-AC8, a Shell Doctoral Fellowship and the P. D. Krynine Fund.

REFERENCES

- ALLEN, J. R. L. (1970) A quantitative model of grain-size and sedimentary structures in lateral deposits. *Geol. J.*, **7**, 129–146.
- ANDERSON, R. Y. (1960) Cretaceous–Tertiary palynology, eastern side of the San Juan Basin, New Mexico. *New Mexico Bureau Mines Mineral Resources, Memoir*, **6**.
- ARMSTRONG, R. L. (1968) The Sevier orogenic belt in Nevada and Utah. *Geol. Soc. Am. Bull.*, **49**, 429–458.
- BARRELL, J. (1925) Marine and terrestrial conglomerates. *Geol. Soc. Am. Bull.*, **36**, 279–342.
- BRAY, D. I. (1982) Regime equations for gravel-bed rivers. In: *Gravel-Bed Rivers* (Ed. by R. D. Hey, J. C. Bathurst and C. R. Thorne), pp. 517–542. Wiley, Chichester.
- BRIDGE, J. S. (1993) Description and interpretation of fluvial deposits: a critical perspective. *Sedimentology*, **40**, 801–810.
- BRIDGE, J. S. & DIEMER, J. A. (1983) Quantitative interpretation of an evolving ancient river system. *Sedimentology*, **30**, 599–623.
- BURBANK, D. W., MEIGS, A. & BROZOVIC, N. (1996) Interactions of growing folds and coeval depositional systems. *Basin Res.*, **8**, 199–223.
- BURBANK, D. W. & VERGÉS, J. (1994) Reconstruction of topography and related depositional systems during active thrusting. *J. geophys. Res.*, **99**, 281–297.
- CROSS, T. A. (1986) Tectonic controls of foreland basin subsidence and Laramide style deformation, western United States. In: *Foreland Basins* (Ed. by P. A. Allen, and P. Homewood), Special Publication Number 8 of the International Association of Sedimentologists, Blackwell, Oxford.
- CUI, Y., PARKER, G. & PAOLA, C. (1996) Numerical simulation of aggradation and downstream fining. *J. Hydraulic Res.*, **34**, 185–204.
- DECELLES, P. G. & GILES, K. A. (1996) Foreland basin systems. *Basin Res.*, **8**, 105–123.
- DECELLES, P. G., LAWTON, T. F. & MITRA, G. (1995) Thrust timing, growth of structural culminations, and synorogenic sedimentation in the type Sevier orogenic belt, western United States. *Geology*, **23**, 699–702.
- FLEMINGS, P. B. & JORDAN, T. E. (1989) A synthetic stratigraphic model of foreland basin development. *J. geophys. Res.*, **94**, 3851–3866.
- FOUCH, T. D., LAWTON, T. F., NICHOLS, D. J., CASHION, W. B. & COBBAN, W. A. (1983) Patterns and timing of synorogenic sedimentation. In: *Upper Cretaceous of Central and Northeast Utah* (Ed. by M. W. Reynolds, M. W. and E. D. Dolly), *Mesozoic paleogeography of west-central United States: Rocky Mountain Section, Soc. Economic Paleontologists Mineralogists, Rocky Mountain Paleogeography Symp.*, **2**, 305–336.
- FRANCZYK, K. J. & PITMAN, J. K. (1991) Latest Cretaceous nonmarine depositional systems in the Wasatch Plateau area: reflections of foreland to intermontane basin transition. In: *Geology of east-central Utah* (Ed. by T. C. Chidsey), *Utah Geol. Assoc. Publ.*, **19**, 77–93.
- FRANCZYK, K. J., PITMAN, J. K. & NICHOLS, D. J. (1990) Sedimentology, mineralogy, palynology, and depositional history of some uppermost Cretaceous and lowermost Tertiary rocks along the Utah Book and Roan Cliffs east of Green River. *United States Geological Survey Bulletin*, **1781-N**.
- GILL, J. R. & HAIL, W. J. JR (1975) Stratigraphic sections across Upper Cretaceous Mancos Shale–Mesaverde Group boundary, eastern Utah and western Colorado. *U. S. Geological Survey Oil and Gas Investigations Chart OC-68, 1 sheet*.
- GUPTA, S. (1997) Himalayan drainage and the origin of fluvial mega fans in the Ganges foreland basin. *Geology*, **25**, 11–14.
- HAQ, B. U., HARDENBOL, J. & VAIL, P. R. (1988) Mesozoic and Cenozoic chronostratigraphy and eustatic cycles. In: *Sea-Level Changes: an Integrated Approach* (Ed. by C. K. Wilgus et al.), *Soc. Econ. Paleont. Miner. Spec. Publ.*, **42**, 71–108.
- HELLER, P. L., BOWDLER, S. S., CHAMBERS, H. P., COOGAN, J. C., HAGEN, E. S., SHUSTER, M. W. & WINSLOW, N. S. (1986) Timing of initial thrusting in the Sevier orogenic belt, Idaho–Wyoming and Utah. *Geology*, **14**, 388–391.
- HELLER, P. L. & PAOLA, C. (1992) The large-scale dynamics of grain-size variation in alluvial basins, 2: Application to syntectonic conglomerate. *Basin Res.*, **4**, 91–102.
- HUVIUS, N. (1996) Regular spacing of drainage outlets from linear mountain belts. *Basin Res.*, **8**, 29–44.
- KAMOLA, D. & VAN WAGONER, J. W. (1995) Stratigraphy and facies architecture of parasequences with examples from the Spring Canyon Member, Blackhawk Formation, Utah. In: *Sequence Stratigraphy of Foreland Basin Deposits – Outcrops and Subsurface Examples from the Cretaceous of North America* (Ed. by J. C. Van Wagoner and G. T. Bertram), *Am. Assoc. Petrol. Geol. Mem.*, **64**, 27–54.
- KODAMA, Y. (1994) Experimental study of abrasion and its role

- in producing downstream fining in gravel-bed rivers. *J. sedim. Res.*, **A64**, 76–85.
- KUENEN, P. H. (1956) Experimental abrasion of pebbles. 2. Rolling by current. *J. Geol.*, **64**, 336–368.
- LAGESON, D. R. & SCHMITT, J. G. (1994) The Sevier orogenic belt of the Western United States: recent advances in understanding its structural and sedimentological framework. In: *Mesozoic systems of the Rocky Mountain region, U.S.A* (Ed. by M. V. Caputo, J. A. Peterson and K. J. Franczyk), pp. 27–64. Rocky Mountain Section of Society of Sedimentary Geology.
- LAWTON, T. F. (1983) Late Cretaceous fluvial systems and the age of foreland uplifts in central Utah. In: *Rocky Mountain Foreland Basins and Uplifts* (Ed. by J. D. Lowell), pp. 181–199. Rocky Mountain Association of Geologists.
- LAWTON, T. F. (1985) Style and timing of frontal structures, thrust belt, central Utah. *Am. Assoc. Petrol. Geol.*, **69**, 1145–1159.
- LAWTON, T. F. (1986a) Fluvial systems of the Upper Cretaceous Mesaverde Group and Paleocene North Horn Formation, central Utah: a record of transition from thin-skinned to thick-skinned thrusting in the foreland region. In: *Paleotectonics and Sedimentation in the Rocky Mountain Region, United States* (Ed. by J. A. Peterson), *Am. Assoc. Petrol. Geol. Mem.*, **41**, 423–442.
- LAWTON, T. F. (1986b) Compositional trends within a clastic wedge adjacent to a fold-thrust belt: Indianola Group, central Utah, USA. In: *Foreland Basins* (Ed. by P. A. Allen and P. Homewood), pp. 411–423. Blackwell, London.
- LAWTON, T. F., BOYER, S. E. & SCHMITT, J. G. (1994) Influence of inherited taper on structural variability and conglomerate distribution, Cordilleran fold and thrust belt, western United States. *Geology*, **22**, 339–342.
- LAWTON, T. F., SPRINKEL, D. A., DECELLES, P. G., MITRA, G., SUSSMAN, A. J. & WEISS, M. P. (1997) Stratigraphy and structure of the Sevier thrust belt and proximal foreland-basin system in central Utah: a transect from the Sevier Desert to the Wasatch Plateau. *Brigham Young University Studies*, **42**, Part II, 33–67.
- LAWTON, T. F., SPRINKEL, D. A. & WAANDERS, G. L. (in press) Continental stratigraphy of the Cretaceous thrust belt and proximal foreland, central Utah. In: *Recent Advances in Understanding the Sevier Orogenic Belt of the Western United States* (Ed. by D. Lageson, and J. A. Schmitt), Geological Society of America Special Paper.
- LAWTON, T. F. & TREXLER, J. H. JR (1991) Piggyback basin development in the Sevier orogenic belt, Utah: implications for development of the thrust wedge. *Geology*, **19**, 827–830.
- LINDHOLM, R. C., HAZLETT, J. M. & FAGIN, S. W. (1979) Petrology of Triassic-Jurassic conglomerate in the Culpeper basin, Virginia. *J. sedim. Res.*, **49**, 1245–1262.
- MACKEY, S. D. & BRIDGE, J. S. (1995) Three-dimensional model of alluvial stratigraphy: theory and application. *J. sedim. Res.*, **B65**, 7–31.
- MIALL, A. D. (1993) The architecture of fluvial-deltaic sequences in the Upper Mesaverde Group (Upper Cretaceous), Book Cliffs, Utah. In: *Braided Rivers* (Ed. by J. L. Best and C. S. Bristow), *Geol. Soc. Special Publ.*, **75**, 305–332.
- MIALL, A. D. (1994) Reconstructing fluvial macroform architecture from two-dimensional outcrops: examples from the Castlegate Sandstone, Book Cliffs, Utah. *J. sedim. Res.*, **B64**, 146–158.
- NEWMAN, K. R. (1965) Upper Cretaceous-Paleocene guide palynomorphs from northwestern Colorado. *University Colorado Studies, Series in Earth Sci.*, **21**.
- NICHOLS, D. J. (1994) A revised palynostratigraphic zonation of the nonmarine Upper Cretaceous, Rocky Mountain region, United States. In: *Mesozoic Systems of the Rocky Mountain Region, U. S. A.* (Ed. by M. V. Caputo, J. A. Peterson and K. J. Franczyk), pp. 503–521. Rocky Mountain Section of Society of Sedimentary Geology.
- NICHOLS, D. J. & JACOBSEN, S. R. (1982) Palynostratigraphic framework for the Cretaceous (Albian-Maestrichtian) of the overthrust belt of Utah and Wyoming. *Palynology*, **6**, 119–147.
- NICHOLS, D. J. & SWEET, A. R. (1993) Biostratigraphy of the Upper Cretaceous non-marine palynofloras in a north-south transect of the Western Interior basin. In: *Evolution of the Western Interior Basin* (Ed. by W. G. E. Caldwell and E. G. Kauffman), *Geol. Assoc. Can. Special Paper*, **39**, 539–584.
- O'BYRNE, C. J. & FLINT, S. (1995) Sequence, parasequences and intrasequence architecture of the Grassy member, Blackhawk Formation, Book Cliffs, Utah, U.S.A. In: *Sequence Stratigraphy of Foreland Basin Deposits – Outcrops and Subsurface Examples from the Cretaceous of North America* (Ed. by J. C. Van Wagoner and G. T. Bertram), *Am. Assoc. Petrol. Geol. Mem.*, **64**, 225–256.
- OBRAĐOVICH, J. D. (1993) A Cretaceous time-scale. In: *Evolution of the Western Interior Basin* (Ed. by W. G. E. Caldwell and E. G. Kauffman), *Geol. Assoc. Can. Special Paper*, **39**, 379–396.
- OLSEN, T., STEEL, R. J., HØGSETH, K., SKAR, T. & RØE, S. (1995) Sequential architecture in a fluvial succession: sequence stratigraphy in the Upper Cretaceous Mesaverde Group, Price Canyon, Utah. *J. sedim. Res.*, **B65**, 265–280.
- PANG, M. (1994) *Tectonic subsidence of the Cretaceous Western Interior Basin*. PhD dissertation, Department of Geology and Geophysics, Louisiana State University.
- PANG, M. & NUMMEDAL, D. (1995) Flexural subsidence and basement tectonics of the Cretaceous Western Interior basin, United States. *Geology*, **23**, 173–176.
- PAOLA, C., HELLER, P. L. & ANGEVINE, C. L. (1992) The large-scale dynamics of grain-size variation in alluvial basins, 1: Theory. *Basin Res.*, **4**, 73–90.
- PARKER, G. (1991) Selective sorting and abrasion of river gravel. II: Applications. *J. Hydraulic Engineering*, **117**, 150–171.
- PFÄFF, B. J. (1985) *Sedimentologic and tectonic evolution of the fluvial facies of the Upper Cretaceous Castlegate Sandstone, Book Cliffs, Utah*. Masters thesis, University of Utah, Salt Lake City, Utah.
- PIZZUTO, J. E. (1995) Downstream fining in a network of gravel-bedded rivers. *Water Resources Res.*, **31**, 753–759.
- RIBA, O. (1976) Syntectonic unconformities of the Alto Cardener, Spanish Pyrenees: a genetic interpretation. *Sediment. Geol.*, **15**, 213–233.
- RICE, S. (in press) Which tributaries disrupt downstream fining along gravel-bed rivers? *Geomorphology*.
- RICE, S. & CHURCH, M. (in press) Grain-size along two gravel-bed rivers: Statistical variation, spatial pattern and sedimentary links. *Earth Surf. Process. Landforms*.
- ROBINSON, R. A. J. (1997) *The origin and significance of grain-size trends in ancient fluvial deposits*. PhD dissertation, Department of Geosciences, Pennsylvania State University.
- ROBINSON, R. A. J. & SLINGERLAND, R. L. (in press) The origin

- of fluvial grain-size trends in a foreland basin: the Pocono Formation of the central Appalachian basin. *J. sedim. Res.*
- ROSS, N. (1949) On a Cretaceous pollen and spore-bearing clay of Scania. *Bull. Geol. Inst., University Uppsala*, **34**, 25–43.
- ROUSE, G. E. (1957) The application of a new nomenclatural approach to Upper Cretaceous plant microfossils from western Canada. *Can. J. Bot.*, **35**, 349–375.
- SAMOILOVICH, S. R. (1967) Tentative botanico-geographical subdivision of northern Asia in Late Cretaceous time. *Rev. Palaeobotany Palynol.*, **2**, 127–139.
- SCHWANS, P. (1995) Controls on sequence stacking and fluvial to shallow-marine architecture in a foreland basin. In: *Sequence Stratigraphy of Foreland Basin Deposits – Outcrops and Subsurface Examples from the Cretaceous of North America* (Ed. by J. C. Van Wagoner and G. T. Bertram), *Am. Assoc. Petrol. Geol. Mem.*, **64**, 55–102.
- SINHA, R. & FRIEND, P. F. (1994) River systems and sediment flux, Indo-Gangetic Plains, Northern Bihar, India. *Sedimentology*, **41**, 825–845.
- SPIEKER, E. M. (1946) Late Mesozoic and early Cenozoic history of central Utah. *United States Geological Survey Professional Paper*, **205-D**, 117–161.
- SPIEKER, E. M. (1949) The transition between the Colorado Plateaus and the Great Basin in central Utah. *Utah Geol. Soc. Guidebook to Geol. Utah*, **4**.
- STERNBERG, H. (1875) Untersuchungen über langen-und querprofil geschieferende flüsse: Zeits. *Baumesen*, **25**, 483–506.
- TUCKER, G. E. & SLINGERLAND, R. L. (1996) Predicting sediment flux from fold and thrust belts. *Basin Res.*, **8**, 329–349.
- VAN DE GRAAFF, F. R. (1972) Fluvial-deltaic facies of the Castlegate Sandstone (Cretaceous), east-central Utah. *J. sedim. Res.*, **42**, 558–571.
- VAN WAGONER, J. C. (1995) Sequence stratigraphy and marine to nonmarine facies architecture of foreland basin strata, Book Cliffs, Utah, U. S. A. In: *Sequence Stratigraphy of Foreland Basin Deposits – Outcrops and Subsurface Examples from the Cretaceous of North America* (Ed. by J. C. van Wagoner and G. T. Bertram), *Am. Assoc. Petrol. Geol. Mem.*, **64**, 137–233.
- VAN WAGONER, J. C., NUMMEDAL, D., JONES, C. R., TAYLOR, D. R., JENNETTE, D. C. & RILEY, G. W. (1991) *Sequence Stratigraphy: Applications to Shelf Sandstone Reservoirs – Outcrop to Subsurface Examples*. American Association of Petroleum Geologists Field Conference Guidebook.
- VILLIEN, A. & KLIGFIELD, R. M. (1986) Thrusting and synorogenic sedimentation in central tah. In: *Paleotectonics and Sedimentation in the Rocky Mountain Region, United States* (Ed. by J. A. Peterson), *Am. Assoc. Petrol. Geol. Mem.*, **41**, 281–307.
- WILLIS, B. (1993) Evolution of Miocene fluvial systems in the Himalayan foredeep though a two kilometer-thick succession in northern Pakistan. *Sediment. Geol.*, **88**, 77–121.
- YOSHIDA, S., MIAL, A. & WILLIS, A. (in press) Sequence stratigraphy and marine to nonmarine facies architecture of foreland basin strata, Book Cliffs, Utah, U.S.A. – Discussion. *Am. Assoc. Petrol. Geol. Bull.*
- YOSHIDA, S., WILLIS, A. & MIAL, A. (1996) Tectonic control of nested sequence architecture in the Castlegate Sandstone (Upper Cretaceous), Book Cliffs, Utah. *J. sedim. Res.*, **66**, 737–748.
- YOUNG, R. G. (1955) Sedimentary facies and intertonguing in the Upper Cretaceous of the Book Cliffs, Utah–Colorado. *Bull. Geol. Soc. Am.*, **66**, 177–202.

Received 5 June 1997; revision accepted 7 January 1998.

Copyright of Basin Research is the property of Wiley-Blackwell and its content may not be copied or emailed to multiple sites or posted to a listserv without the copyright holder's express written permission. However, users may print, download, or email articles for individual use.